Accuracy of gastrocnemius muscles forces in walking and running goats predicted by one-element and two-element Hill-type models

Sabrina S.M. Lee[1], **Allison S. Arnold**[2], **Maria de Boef Miara**[2], **Andrew A. Biewener**[2], and **James M. Wakeling**[1]

[1]Department of Biomedical Physiology and Kinesiology, Simon Fraser University, Burnaby, BC, Canada

[2]Concord Field Station, Harvard University, Bedford, MA, USA

Abstract

Hill-type models are commonly used to estimate muscle forces during human and animal movement —yet the accuracy of the forces estimated during walking, running, and other tasks remains largely unknown. Further, most Hill-type models assume a single contractile element, despite evidence that faster and slower motor units, which have different activation-deactivation dynamics, may be independently or collectively excited. This study evaluated a novel, two-element Hill-type model with "differential" activation of fast and slow contractile elements. Model performance was assessed using a comprehensive data set (including measures of EMG intensity, fascicle length, and tendon force) collected from the gastrocnemius muscles of goats during locomotor experiments. Muscle forces predicted by the new two-element model were compared to the forces estimated using traditional one-element models and to the forces measured *in vivo* using tendon buckle transducers. Overall, the two-element model resulted in the best predictions of *in vivo* gastrocnemius force. The coefficient of determination, r^2, was up to 26.9% higher and the root mean square error, RMSE, was up to 37.4% lower for the two-element model than for the one-element models tested. All models captured salient features of the measured muscle force during walking, trotting, and galloping ($r^2 = 0.26$ to 0.51), and all exhibited some errors (RMSE = 9.63 to 32.2% of the maximum *in vivo* force). These comparisons provide important insight into the accuracy of Hill-type models. The results also show that incorporation of fast and slow contractile elements within muscle models can improve estimates of time-varying, whole muscle force during locomotor tasks.

Corresponding author: s-lee@northwestern.edu.

Conflict of interest statement
There are no conflicts of interest.

Introduction

Muscle models that accurately reproduce time-varying muscle forces are crucial for evaluating motor performance and key to interpreting muscle-driven simulations of movement. Hill-type models, which estimate a muscle's force based on length-tension and force-velocity properties (e.g., Zajac, 1989; Winters, 1990), are arguably one of the most widely-used tools in biomechanics — yet the accuracy of the forces predicted by Hill-type models during walking, running, and other motor tasks remains largely unknown. In this study, we examined the ability of several different Hill-type models to reproduce *in vivo* gastrocnemius forces measured in goats during locomotion.

Rigorous validation of Hill-type models requires experimental measures of fascicle lengths and muscle excitations, which are typically used to drive the models, as well as direct measures of muscle or tendon force. Most previous tests of muscle models have relied on *in situ* stimulation experiments in animals, where the neural excitation and fascicle strain values are not generally representative of *in vivo* dynamic behavior (e.g., Brown and Loeb, 1999, 2000). Only a few studies have assessed the performance of Hill-type models under more realistic conditions (Sandercock and Heckman, 1997; Perreault et al., 2003). Varying results in the errors in force prediction by muscle models, and the paucity of validation studies based on *in vivo* data, warrant further investigation. In particular, models must be tested during dynamic tasks that involve time-varying excitations, both to refine interpretation and to identify limitations that need to be addressed.

One limitation of traditional Hill-type models is their failure to account for different mechanical properties of the fiber types recruited. Muscles are comprised of different types of muscle fibers, broadly classified as slow to fast, that have different activation-deactivation rates, and force development. Most previous Hill-type models assume either that fiber type within the muscle is homogeneous (e.g., Zajac, 1989) or that orderly recruitment occurs (e.g. Umberger et al. 2003; van Soest and Bobbert, 1993). However, previous analyses of motor unit recruitment in rats (Hodson-Tole and Wakeling, 2009), humans (Wakeling 2004), and goats (Lee et al., 2013) have revealed that the recruitment patterns of slow and fast fibers can vary depending on the motor task. Recently, we showed that a Hill-type model could more accurately predict gastrocnemius forces in goats during *in situ* isometric contractions when the model incorporated both fast and slow contractile elements, and when the contractile elements were activated in a manner consistent with measured electromyographic (EMG) recordings (Wakeling et al. 2012). Some other muscle models have incorporated different fiber-type properties, but have also been limited to simulations of isometric contractions (Bol et al., 2011; Fuglevand et al., 1993). Therefore, a secondary aim of this study was to test — for *in vivo* locomotor tasks — whether a Hill-type model with fast and slow contractile elements (i.e., a "two-element model" or "differential" model) yields more accurate predictions of whole muscle force than traditional one-element

models. We compared our recently developed, two-element model (Wakeling et al. 2012) to three commonly used Hill-type models that have been applied in a wide range of biomechanics applications. *In situ* and *in vivo* experiments were conducted on the lateral and medial gastrocnemius (LG and MG) muscles of goats, as these muscles are known to comprise both slow and fast fibers (Lee et al., 2013). These experiments yielded simultaneous recordings of fascicle length, excitation, and time-varying tendon force, providing a comprehensive and informative data set for testing the predictive accuracy of the different models. The models in this study relied on measured fascicle lengths, rather than on scaled fiber lengths derived from the muscle-tendon lengths (e.g., Zajac et al., 1989); this allowed us to evaluate modeling assumptions related to properties of the fiber types recruited, which was our main goal, while minimizing uncertainty in the models' force-length properties, which also influence the predicted force.

Methods

Six African pygmy goats (*Capra hircus* L; 3 males, 3 females; age 21.0 ± 15.5 months, mass 25.85 ± 6.20 kg) were tested at Harvard University's Concord Field Station. The experimental protocol involved four main steps over a three-day period: surgical implantation of transducers, *in vivo* testing, surgical implantation of nerve cuffs, and *in situ* testing. All experimental protocols are described elsewhere (Lee et al., 2011, Wakeling et al., 2012, Lee et al., 2013; also see supplementary materials) and are reviewed here in brief:

Experimental data collection

1. Goats were trained to walk, trot and gallop on a motorized treadmill, and they performed these gaits on level and inclined surfaces as part of a larger study. Our previous analysis showed that the level trials elicited the most pronounced differences in recruitment (Lee et al., 2013). Thus, the level trials were used in the current study to test the different muscle models.

2. The MG and LG were instrumented with fine-wire EMG electrodes to measure muscle excitation (Lee et al., 2011), sonomicrometry crystals to measure fascicle length (resolution = 0.3μm Lee et al., 2011), and "E"- shaped tendon buckle transducers on the Achilles tendon were used to measure tendon force (calibration yielded $r^2 > 0.99$, Biewener & Baudinette, 1995). *In vivo* lateral and medial tendon forces were estimated from the total *in vivo* tendon force, measured by the single tendon buckle on the tendon, using the ratio of the maximum forces measured from the *in situ* recordings of the lateral and medial gastrocnemius muscles from the two tendon buckles (see below). Tendon forces were normalized by the maximum force recorded during incline trotting, F_{max}, consistent with previous analyses (Lee et al., 2013).

3. *In vivo* recordings were made while goats walked, trotted, and galloped on the treadmill. Between 15 and 20 strides were recorded for each condition, and data were recorded at 5000 Hz (Lee et al., 2013). Sufficient rest was given between trials to ensure the goats could complete the experiments.

4. An additional force transducer was surgically attached on the medial portion of the Achilles tendon prior to the *in situ* experiments. *In situ* recordings were made to measure the muscles' active and passive force-length relationships, using tetanic stimulation, for a range of ankle angles and muscle lengths. A series of different nerve stimulation protocols were used to elicit twitches from different motor units, enabling identification of the twitch profiles for slow and fast motor units (Lee et al., 2011).

Experimental data processing

5 To extract information about motor unit recruitment that could be used to drive the muscle models, the major components of the EMG signal corresponding to signals from slow and fast motor units were identified using wavelet analysis (von Tscharner, 2000; Lee et al., 2011). Optimized wavelets were derived to identify recruitment patterns of slow and fast motor units (Lee et al., 2011; Wakeling, 2005; Hodson-Tole and Wakeling, 2008). The EMG signal was characterized by its total intensity and by the intensities at the low- and high-frequency bands, corresponding to signals from the whole muscle and from slower and faster motor units, respectively (Fig. 1). The final step in the intensity calculation was applying a Gauss filter to the intensity envelope. The filter width was set to have the same time resolution (75 ms) for all measures of intensity so that temporal-based comparisons could be made between the different models (see Supplementary Material for more details).

6 The EMG intensities were used as excitations for a series of coupled first-order differential equations, constituting transfer functions (Eq. 1), that enabled estimation of the active state of each muscle. Transfer functions were derived for the whole muscle as well as for the slower and faster motor units (Figures 1 and 2; Lee et al., 2011); in particular, constants $\tau_{act1,2,3}$ and $\beta_{1,2,3}$ were identified for the different motor units (Table 1) and were determined from *in situ* data pooled from the six goats. Details are described elsewhere (see supplementary materials, Lee et al., 2011).

$$\frac{d}{dt}(a_1) + \left[\frac{1}{\tau_{act1}} (\beta_1 + [1 - \beta_1] EMG(t - t_{off})) \right] a_1(t) = \left(\frac{1}{\tau_{act1}} \right) EMG(t - t_{off})$$
$$\frac{d}{dt}(a_2) + \left[\frac{1}{\tau_{act2}} (\beta_2 + [1 - \beta_2] a_1(t)) \right] a_2(t) = \left(\frac{1}{\tau_{act2}} \right) a_1(t) \qquad \text{(Eq.1)}$$
$$\frac{d}{dt}(a_3) + \left[\frac{1}{\tau_{act3}} (\beta_3 + [1 - \beta_3] a_2(t)) \right] a_3(t) = \left(\frac{1}{\tau_{act3}} \right) a_2(t)$$

Activation levels of the slower and faster motor units were scaled in amplitude such that summation of the two levels equaled the activation level of the whole muscle (i.e., the total activation, Figure 2). This simplified comparison of the one-element and two-element models.

Muscle Models

Three one-element muscle models and a novel two-element model (Wakeling et al. 2012) were used to estimate time-varying forces produced by the MG and LG during the different

locomotor conditions (Figure 1). The three one-element models generated similar predictions of muscle force so only one is presented here; the other one-element models are described in the supplementary material. The output of each model, the total muscle force F_m, was estimated by:

$$F_m = c \left[\hat{F}_f + \hat{F}_p(l) \right] \, cos\theta \quad \text{(Eq. 2)}$$

where $\hat{F_f}$ is the active component of the muscle fiber force and $\hat{F_p}$ is the passive component of the force as a function of fiber length (l). Constant c and the pennation angle, θ, scaled the fiber force to the whole muscle force. In particular, constant c scaled the predicted force from its normalized value to the measured force for each goat. Thus, c reflects the maximum isometric force generated by the muscle. The pennation angle was calculated at each time step as a function of fiber length (l) from the resting pennation angle and the fascicle length, assuming that the thickness of the muscle remained constant (Zajac, 1989; Millard and Delp, 2012; van den Bogert et al., 2011; see Table 2 for mean and standard deviation values of optimal and resting fascicle length and pennation angle). The inputs to each model included the time-varying fascicle lengths, which were also used to calculate fiber contractile velocity and pennation angle, and the activation states (Figures 1 and 2). The activation states were normalized to the maximum activation during incline trotting, consistent with our procedure for normalizing the measured tendon forces. Other parameters used in the models (Figure 1 and Table 3) were either derived from experimental measurements or taken from the literature, and were not optimized to "fit" the *in vivo* forces.

For the one-element models, the active component of the muscle fiber force was given by:

$$\hat{F}_f = \hat{a}(t) \, \hat{F}_a(l) \, \hat{F}_\nu(\nu) \quad \text{(Eq. 3)}$$

where $\hat{a}(t)$ is the time-varying activation level (Lee et al., 2011) and $\hat{F_a}(l)$ is the active force-length relationship normalized to maximum of 1. The active (Eq. 4) and passive (Eq. 5) force-length curves were based on *in situ* measurements, taken during supramaximal stimulation, at a range of fascicle lengths. These equations were derived by fitting the *in situ* data pooled from all goats.

$$\hat{F}_a(l) = \frac{((-878.25 \, (l * 1.253)^2 + 2200.4 \, (l * 1.254) - 1192)}{186.24} \quad \text{(Eq.4)}$$

$$\hat{F}_p(l) = \frac{e^{-1.3 + 3.8 * (l * 1.253)}}{186.24} \quad \text{(Eq.5)}$$

The force-velocity relationship, $\hat{F_\nu}(\nu)$, was given by:

$$\hat{F}_\nu(\nu) = \frac{\left(1 - \frac{\nu}{\nu_o}\right)}{\left(1 + \frac{\nu}{\nu_o k}\right)} \, for \; \nu \leq 0 \quad \text{(Eq. 6)}$$

$$\hat{F}_\nu (\nu) = 1.5 - 0.5 \frac{\left(1 + \frac{\nu}{\nu_0}\right)}{\left(1 - \frac{7.56\nu}{\nu_o k}\right)} \text{ for } \nu > 0 \quad \text{(Eq. 7)}$$

where ν is the fiber contractile velocity, ν_0 is the maximum intrinsic speed, and constant k characterizes the curvature of the force-velocity curve. Note that shortening velocity is defined as negative in these equations, while lengthening is defined as positive. ν_0 is presented as a positive value, but it is implemented as a negative value in Eqs. 6 and 7. Different values of ν_0 and k were assigned for the different models, based on assumptions about motor unit recruitment, as described in the following sections.

The one-element model presented here presumed that active muscles display intrinsic properties of progressively faster fiber types as activation levels increase. Thus, at initial low activation levels, the active fibers were assigned a maximum unloaded shortening velocity corresponding to slow fibers (Table 4). As activation levels increased, the maximum shortening velocity also increased. This model is based on classical studies of orderly recruitment during steady stretch reflexes (Hennemen, 1974) and is consistent with previous muscle modeling approaches (e.g. Umberger et al., 2003; Van Soest et al., 1993). Two sets of values representing the maximum unloaded shortening velocities of the slower and faster fibers were tested; this is because previous studies have shown that muscle models are generally sensitive to this parameter (Wakeling et al., 2012). The values we used were (a) 2.74 and 3.59 l_{opt} s^{-1} for the slower and faster motor units, respectively, estimated from *in situ* measures of activation rates scaled by literature values across a range of species, and (b) 5 and 10 l_{opt}s^{-1} for the slow and fast fibers, respectively, based on previous models of larger species (Wakeling et al., 2012). Constant k, which characterizes the curvature of the force-velocity curve, was assigned an intermediate value within the ranges of the slow and fast fibers; we used values of 0.18 and 0.29 for slow and fast fibers, respectively (Wakeling et al., 2012). For the one-element model, curvature k was assumed to be the same for all the fibers within the muscle (Table 4). Since p, the fractional area of the fast fibers, remains unknown for goats, two different values were tested. We used values of 0.75 and 0.5 since our initial immunohistochemical testing of the LG and MG in goats has shown that the LG contains a proportion of fast fibers within this range (unpublished observations, Carr, Miara, Lee, Wakeling, and Biewener).

The two-element differential recruitment model (Figure 1) incorporated independently-activated slow and fast contractile elements in parallel (Wakeling et al., 2012). The EMG intensities at the low- and high- frequency bands were used with the transfer functions (Eq. 1 and Table 1) to estimate the activation levels for the slow and fast elements, $\hat{a}_{slow}(t)$ and $\hat{a}_{fast}(t)$ respectively. The total active force from the fibers, $\hat{F_f}$, was given by:

$$\hat{F}_f = \hat{F}_{f,slow} + \hat{F}_{f,fast} \quad \text{(Eq.8)}$$

where $\hat{F}_{f,slow}$ and $\hat{F}_{f,fast}$ are the normalized forces for slow and fast fibers, respectively, as determined from Equation 3 using fiber-specific values of $\hat{a}(t)$, ν_0, and k (Tables 3 and 4).

Comparisons of predicted and measured forces

Simulations were run for the different models, goats, muscles, and gait conditions, varying the values of p and v_0. Differences between the predicted force and the measured force were characterized by the coefficient of determination, r^2, and by the root mean square error, RMSE. These measures were useful for quantitatively comparing the accuracy of the time-varying forces predicted by each model. A general linear model ANOVA was conducted to determine if differences in the r^2 and RMSE values existed between the different models, muscles, gait conditions, fiber-type proportions, and v_0 values. Differences were considered significant at the $\alpha = 0.05$ level. Tukey post-hoc analyses were conducted to identify significant differences between levels within a factor when indicated.

Results

The two-element model and all of the one-element models that we tested generally captured the detailed changes in the measured gastrocnemius forces during walking, trotting, and galloping. However, all models exhibited some errors that included inaccurate estimates of the peak force and insufficient rates of force rise and decline (e.g., Figure 3). Across all models, the coefficient of determination values ranged from 0.32 to 0.51 for the LG and from 0.26 to 0.48 for the MG (Figure 4). The RMSE, as a percentage of the maximum *in vivo* force measured during incline trotting, ranged from 17.0 % to 32.2 % for the LG and from 9.63 % to 15.5 % for the MG (Figure 4). Importantly, the different gait conditions tested the models over a physiological range of force amplitudes and contraction speeds.

The two-element muscle model generally performed better than the one-element models. In particular, the differential model predicted time-varying LG forces with significantly statistically higher r^2 (better correlation) and lower RMSE (less error) than the one-element model described here, both during galloping (r^2, p = 0.03; RMSE, p = 0.001; Figures 2-4) and during trotting (RMSE, p < 0.001). The differential model also predicted time-varying MG forces with significantly lower RMSE than the one-element model during trotting and galloping (p = 0.001 and p = 0.01, Figure 4).

Results of the ANOVA revealed that the accuracy of the predicted *in vivo* force was dependent on muscle, gait, and the choice of v_0 (Figs. 2 to 5). The models generally predicted force more accurately for the MG than for the LG, with higher r^2 and lower RMSE for walking and galloping (p < 0.001). Adjusting the fiber-type proportion (50 % fast versus 75% fast) did not appreciably alter forces predicted by the one-element model. However, adjusting v_0 significantly influenced the accuracy of the predicted LG forces (r^2, p < 0.001, Fig. 5). When v_0 was assigned the faster values of 5 and 10 l_{opt} s^{-1}, the models predicted *in vivo* force better (higher r^2) than when v_0 was assigned the slower values of 2.74 l_{opt} s^{-1} and 3.59 l_{opt} s^{-1}. The performance of the models also differed significantly across the gait conditions (r^2, p < 0.001; RMSE, p < 0.001; Figures 3 to 4).

Discussion

This study examined the accuracy with which a novel, two-element Hill-type model and several commonly-used one-element models predict time-varying forces generated by goat

gastrocnemius muscles during locomotion (see supplementary materials for detailed assessments of the other one-element models). Our comparisons of the predicted and measured forces – based on a comprehensive and unique data set from *in vivo* and *in situ* experiments – provide evidence that Hill-type models can reproduce key features of whole muscle force. However, across locomotor conditions, the models generated errors ranging from 9.63 % to 32.2 % (RMSE as a percentage of the maximum *in vivo* force) when averaged across goats and trials. These errors included inaccuracies in magnitude and timing. Our two-element differential model, in which slow and fast contractile elements are activated independently, generally predicted muscle forces more accurately than the one-element models tested, particularly at the faster gaits (Figures 3 and 4). The r^2 increased from 0.37 to 0.43 (mean across gaits) for the LG, and the RMSE decreased from 25.3 % to 17.2 % (percent of maximum measured force) for the LG and from 13.2 % to 11.5 % for the MG.

Activation dynamics

The main difference, and perhaps the most informative difference, between the two-element differential model and the three one-element models tested was our calculation of the active state used to drive the contractile element(s). Specifically, the differential model was driven by the active states of independent slow and fast fibers acting in parallel (Figures 1 and 2). While differences in the muscle forces predicted by the one- and two-element models during goat locomotion were not dramatic, we believe they are large enough to be relevant. Experimental data from rats (Hodson-Tole and Wakeling, 2009), humans (Wakeling 2004), and goats (Lee et al., 2013) have shown that the different motor unit types can be recruited in a task-specific fashion varying, for example, with changes in fascicle strain rates that accompany changes in locomotor speed. Thus, the two-element model may be particularly relevant when estimating muscle forces during rapid or explosive movements, when accounting for the recruitment patterns and properties of fast motor units is likely to yield substantial improvements. The two-element model is also likely to be helpful when evaluating muscle force generation in individuals with neuromuscular disorders, who frequently exhibit altered or impaired motor unit recruitment. Our two-element model characterizes the sequence in which these motor unit populations are activated (Coggshall and Bekey, 1970) and, as a result, offers the potential to better predict force development across different motor tasks.

Intrinsic properties

Previous *in situ* studies of Hill-type models have demonstrated that errors in predicted forces are often related to the force-velocity properties assumed (Perreault et al., 2003; Shue et al., 1995). In this *in vivo* study, we also observed that force-velocity properties influenced the accuracy of the muscle forces predicted (Table 4). Values chosen for the maximum shortening velocity, v_0, and the proportion of fast fibers, p, dictated the force-velocity properties of the different models (Eqs. 6-7). Assigning p different values between 50% and 75% did not substantially influence the performance of the models, however, assigning v_0 to have slower (2.74 and 3.59 l_{opt} s^{-1}) or faster (5 and 10 l_{opt} s^{-1}) values did significantly affect force prediction. This suggests that efforts to more accurately characterize a muscle's force-

velocity properties, by experimentation or optimization, could significantly improve the accuracy of Hill-type models.

The MG and LG muscles are known to vary in architecture, fiber composition, and intrinsic motor unit properties (Wakeling et al., 2011, Maganaris et al., 1998), and these differences between the muscles may explain why the models predicted force more accurately for the MG than for the LG. In both man and goats, it is thought that the MG and LG have different activation-deactivation dynamics due to different motor unit twitch profiles (Lee et al., 2011; Vandervoot and McComas, 1983).

Pennation angle is sometimes assumed to be constant in muscle models. However, pennation angle has been shown to change up to 28° from rest to maximum voluntary contraction within human gastrocnemius muscles (Maganaris et al., 1998). By allowing pennation angle to vary as a function of fascicle length in our models, we observed that the timing of the predicted forces was notably improved.

Limitations

One of the aims of this study was to examine the ability of current and commonly used Hill-type models to accurately reproduce muscle forces measured *in vivo*. Despite the improvements achieved by incorporating slow and fast contractile elements into Hill-type models, all of models evaluated in this study have limitations that may have contributed to the errors in magnitude and timing. These limitations include, for example, the assumption that activation, force-length, and force-velocity properties are independent and the failure of these models to account for history-dependent effects (see supplementary materials for detailed discussion). In many of the simulations, we observed errors in relative phasing between the predicted and measured forces in which the predicted force developed earlier than the *in vivo* force. Factors contributing to these errors include the time resolution of the Gauss filter applied in the wavelet analysis and the exclusion of a tendon in the models (see supplementary materials for detailed discussion).

Validation

We previously evaluated the accuracy of MG and LG forces predicted by our two-element model during *in situ* experiments (Wakeling et al., 2012). The comparisons with *in situ* forces yielded higher r^2 values (0.8-0.95) than the comparisons with *in vivo* forces reported here. However, comparisons of the differences in r^2 and RMSE values between the one-element and two element models reveal that the two-element model predicted force more accurately than the one-element model under *in situ* and *in vivo* conditions (Figures 3-4). Under *in situ* and *in vivo* conditions, the r^2 value was up to 9.7% and 37.4% higher, respectively, for the two-element model than for the one-element models tested (RMSE was 32.2% lower; see supplementary materials for more details).

Very few studies have validated Hill-type models under functionally relevant conditions. Many studies have evaluated models based on *in situ* data, but these tests have generally been performed under laboratory conditions where fascicle lengths and activations are not typical of those observed *in vivo* (Perreault et al., 2003; van Ingen Schenau et al., 1998;

Sandercock and Heckman, 1997; see supplementary materials for more detailed discussion). A strength of the current study is that inputs driving the models, along with most parameters, were based on experimental measures from the same set of muscles from which force was measured *in vivo*. Thus, the errors reported here for *in vivo* locomotor tasks are especially informative – revealing the strengths and weaknesses of Hill-type models under physiologically relevant conditions.

Supplementary Material

Refer to Web version on PubMed Central for supplementary material.

Acknowledgments

References

Balnave CD, Allen DG. The effect of muscle length on intracellular calcium and force in single fibers from mouse skeletal muscle. Journal of Physiology. 1996; 492:705–713. [PubMed: 8734983]

Biewener A, Baudinette R. In vivo muscle force and elastic energy storage during steady-speed hopping of tammar wallabies (Macropus eugenii). Journal of Experimental Biology. 1995; 198:1829–41. [PubMed: 9319738]

Bol M, Sturmat M, Weichert C, Kober C. A new approach for the validation of skeletal muscle modeling using MRI data. Computer Mech. 2011; 47:591–601.

Brown IE, Cheng EJ, Loeb GE. Measured and modeled properties of mammalian skeletal muscle. II. The effects of stimulus frequency on force-length and force-velocity relationships. Journal of Muscle Research and Cell Motility. 1999; 20:627–643. [PubMed: 10672511]

Brown IE, Loeb GE. Measured and modeled properties of mammalian skeletal muscle: IV. Dynamics of activation and deactivation. Journal of Muscle Research and Cell Motility. 2000; 21:33–47. [PubMed: 10813633]

Close RI. The relations between sarcomere length and characteristics of isometric twitch contractions of frog sartorius muscle. Journal of Physiology. 1972; 220:745–762. [PubMed: 4536939]

Coggshall JC, Bekey GA. EMG-force dynamics in human skeletal muscle. Medical and Biological Engineering. 1970; 8:265–270. [PubMed: 5491714]

Edman KA, Caputo C, Lou F. Depression of tetanic force induced by loaded shortening of frog muscle fibers. Journal of Physiology. 1993; 466:535–552. [PubMed: 8410705]

Edwards, RHT. Human muscle function and fatigue. In: Porter, R.; Whelan Human, J., editors. Muscle Fatigue: Physiological Mechanisms. John Wiley and Sons, Ltd.; Chichester, UK: 1981. p. 1-18.

Ekelund MC, Edman KA. Shortening induced deactivation of skinned fibers of frog and mouse striated muscle. Acta Physiologica Scandinavica. 1982; 116:189–199. [PubMed: 6820231]

English AW, Letbetter WD. A histochemical analysis of identified compartments of cat lateral gastrocnemius muscle. Anatomical Record. 1982; 204:123–30. [PubMed: 7181128]

Epstein, M.; Herzog, W. Theoretical models of skeletal muscle. John Wiley and Sons; 1998.

Farina D, Fosci M, Merletti R. Motor unit recruitment strategies investigated by surface EMG variables. Journal of Applied Physiology. 2002; 2:235–247. [PubMed: 11744666]

Fuglevand AJ, Winter DA, Patla AE. Models of recruitment and rate coding organization in motor-unit pools. Journal of Neurophysiology. 1993; 92:235–247.

Gardiner PF. Effects of exercise training on components of the motor unit. Canadian Journal of Sport Sciences. 1991; 16:271–288. [PubMed: 1663829]

Gerritsen KG, Nachbauer W, van den Bogert AJ. Computer simulation of landing movement in downhill skiing: anterior cruciate ligament injuries. Journal of Biomechanics. 1996; 29:845–854. [PubMed: 8809615]

Henneman A, Clamann HP, Gillies JD, Skinner RD. Rank order of motorneurons within a pool, law of combination. Journal of Neurophysiology. 1974; 37:1338–1349. [PubMed: 4436704]

Hill, AV. First and Last Experiments in Muscle Mechanics. Cambridge University Press; Cambridge: 1970.

Hodson-Tole EF, Wakeling JM. Variations in motor unit recruitment patterns occur within and between muscles in the running rat (Rattus norvegicus). Journal of Experimental Biology. 2007; 210:2333–45. [PubMed: 17575038]

Hodson-Tole EF, Wakeling JM. Motor unit recruitment patterns 2: the influence of myoelectric intensity and muscle fascicle strain rate. Journal of Experimental Biology. 2008; 211:1893–902. [PubMed: 18515719]

Hodson-Tole E, Wakeling JM. Motor unit recruitment for dynamic tasks: current understanding and future directions. Journal of Comparative Physiology B. 2009; 179:57–66.

Joyce GS, Rack PMH, Westbury DR. Mechanical properties of cat soleus muscle during controlled lengthening and shortening movements. Journal of Physiology. 1969; 204:461–474. [PubMed: 5824647]

Karlsson S, Yu J, Akay M. Time-frequency analysis of myoelectric signals during dynamic contractions: a comparative study. IEEE transactions on bio-medical engineering. 2000; 47:228–38. [PubMed: 10721630]

Kumar DK, Pah ND, Bradley A. Wavelet analysis of surface electromyography. Neural Systems and Rehabilitation Engineering. IEEE Transactions. 2003; 11:400–6.

Lee SSM, de Boef Miara M, Arnold AS, Biewener AA, Wakeling JM. EMG analysis for determining the timing and level of activation in different motor units. Journal of Electromyography and Kinesiology. 2011; 21:557–565. [PubMed: 21570317]

Lee SSM, de Boef Miara M, Arnold-Rife A, Biewener AA, Wakeling JM. Recruitment of faster motor units is associated with greater rates of fascicle strain and rapid changes in muscle force during locomotion. Journal of Experimental Biology. 2013; 216:198–207. [PubMed: 22972893]

Levin O, Mizrahi J, Isakov E. Transcutaneous FES of paralyzed quadriceps: is knee torque affected by unintended activation of the hamstrings. Journal of Electromyography and Kinesiology. 1999; 10:47–58. [PubMed: 10659449]

Lexell J. Ageing and human muscle: observations from Sweden. Canadian Journal of Applied Physiology. 1993; 18:2–18. [PubMed: 8471991]

Maganaris CN, Baltzopoulos V, Sargeant AJ. In vivo measurements of the triceps surae complex architecture in man: implications for muscle function. Journal of Physiology. 1998; 513:603–614. [PubMed: 9763648]

Millard, M.; Delp, S. A computationally efficient muscle model. Proceedings of the ASME 2012 Summer Bioengineering Conference; 2012.

Morgan DL. New insights into the behavior of muscle during active lengthening. Biophysical Journal. 1990; 57:209–221. [PubMed: 2317547]

Perreault EJ, Heckman CJ, Sandercock TG. Hill muscle model errors during movement are greatest within the physiologically relevant range of motor unit firing rates. Journal of Biomechanics. 2003; 36:211–218. [PubMed: 12547358]

Rack PMH, Westbury DR. The effects of length and stimulus rate on tension in the isometric cat soleus muscle. Journal of Physiology. 1969; 204:443–460. [PubMed: 5824646]

Rassier DE, Herzog W, Wakeling J, Syme DA. Stretch-induced, steady-state force enhancement in single skeletal muscle fibers exceeds the isometric force at optimum fiber length. Journal of Biomechanics. 2003; 36:1309–1316. [PubMed: 12893039]

Ralsonton JJ, Todd FN, Inman VT. Comparison of electrical activity and duration of tension in human rectus femoris muscles. Electromyography and Clinical Neurophysiology. 1976; 16:271–278. [PubMed: 964204]

Roszek B, Baan GC, Huijing PA. Decreasing stimulation frequency-dependent length-force characteristics of rat muscle. Journal of Applied Physiology. 1994; 77:2115–2124. [PubMed: 7868423]

Sandercock TG, Heckman CJ. Force from cat soleus muscle during imposed locomotor-like movements: experimental data versus Hill-type model predictions. Journal of Neurophysiology. 1997; 77:1538–1552. [PubMed: 9084618]

Sandercock TG, Heckman CJ. Whole muscle length-tension properties vary with recruitment and rate modulation in a reflexive cat soleus. Journal of Neurophysiology. 2001; 85:1033–1038. [PubMed: 11247973]

Shue G, Crago E, Chizeck HJ. Muscle-joint models incorporating activation dynamics, moment-angle, and moment-velocity properties. IEEE Transactions on Biomedical Engineering. 1995; 42:212–223. [PubMed: 7868149]

Spaegele T, Kistner A, Gollhofer A. Modelling simulation and optimization of human vertical jump. Journal of Biomechanics. 1999; 32:521–30. [PubMed: 10327006]

Stephenson DG, Wendt IR. Length dependence of changes in sarcoplasmic calcium concentration and myofibrilar calcium sensitivity in striated muscle fibers. Journal of Muscle Research and Cell Motility. 1984; 5:243–272. [PubMed: 6378970]

Umberger BR, Gerritsen KGM, Martin PE. A model of human muscle energy expenditure. Computer Methods in Biomechanics and Biomedical Engineering. 2003; 6:99–111. [PubMed: 12745424]

van den Boger A, Blana D, Heinrich D. Implicit methods for efficient musculoskeletal simulation and optimal control. Procedia IUTAM. 2011; 2:297–316. [PubMed: 22102983]

Van Ingen Schenau GJ, Bobbert MF, Ettema GJ, de Graaf JB, Huijing PA. A simulation of rat edl force output based on intrinsic muscle properties. Journal of Biomechanics. 1988; 21:815–824. [PubMed: 3225268]

Van Leeuwen, JL. Muscle function in locomotion. In: McNeil Alexander, R., editor. Mechanics of Animal Locomotion. Springer-Verlag; Berlin: p. 191-250.

Van der Helm, FCT. Large-scale musculoskeletal systems: sensorimotor integration and optimization. In: Winters, JM.; Crago, PE., editors. Biomechanics and Neural Control of Posture and Movement. Springer; New York: 2000. p. 407-424.

Vandervoort AA, McComas AJ. A comparison of the contractile properties of the human gastrocnemius and soleus muscles. European Journal of Applied Physiology. 1983; 51:435–440.

Van Soest AJ, Bobbert MF. The contribution of muscle properties in the control of explosive movements. Biological Cybernetics. 1993; 69:195–204. [PubMed: 8373890]

Von Tscharner V. Intensity analysis in time-frequency space of surface myoelectric signals by wavelets of specified resolution. Journal of Electromyography and Kinesiology. 2000; 10:433–445. [PubMed: 11102846]

von Tscharner V. Time-frequency and principal-component methods for the analysis of EMGs recorded during a mildly fatiguing exercise on a cycle ergometer. J Eletromyography Kinesiology. 2002; 12:479–492.

von Tscharner V, Goepfert B. Estimation of the interplay between groups of fast and slow muscle fibers of the tibialis anterior and gastrocnemius muscle while running. J Electromyography Kinesiology. 2006; 16:188–197.

Wakeling JM, Kaya M, Temple GK, Johnston W, Herzog W. Determining patterns of motor recruitment during locomotion. Journal of Experimental Biology. 2002; 205:359–369. [PubMed: 11854372]

Wakeling JM, Rozitis AI. Spectral properties of myoelectric signals from different motor units in the leg extensor muscles. Journal of Experimental Biology. 2004; 207:2519–28. [PubMed: 15184523]

Wakeling JM. Patterns of motor unit recruitment can be determined using surface EMG. Journal of Electromyography and Kinesiology. 2009; 207:3883–3890.

Wakeling JM, Uehli K, Rozitis AI. Muscle fibre recruitment can respond to the mechanics of the muscle contraction. Journal Royal Society Interface. 2006; 3:533–544.

Wakeling JM, Lee SSM, de Boef Miara M, Arnold AS, Biewener AA. A muscle's force depends on the recruitment patterns of its fibers. Annals of Biomedical Engineering. 2012; 40:1708–1720. [PubMed: 22350666]

Winters, JM. Hill-based muscle models: a systems engineering perspective. In: Winters, JM.; Woo, SL., editors. Multiple Muscle Systems: Biomechanics and Movement Organization. Springer; New York: 1990. p. 69-93.

Zajac FE. Muscle and tendon: properties, models, scaling, and application to biomechanics and motor control. Critical reviews in biomedical engineering. 1989; 17:359–411. [PubMed: 2676342]
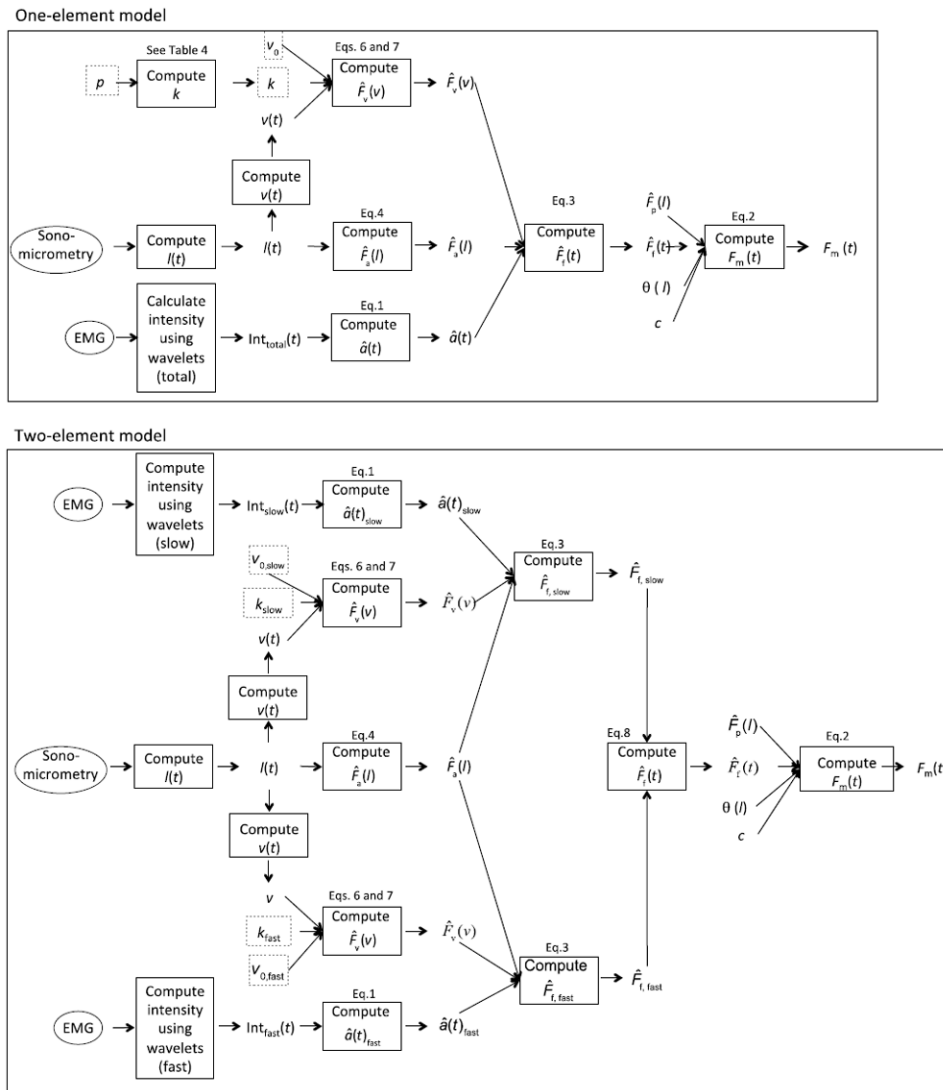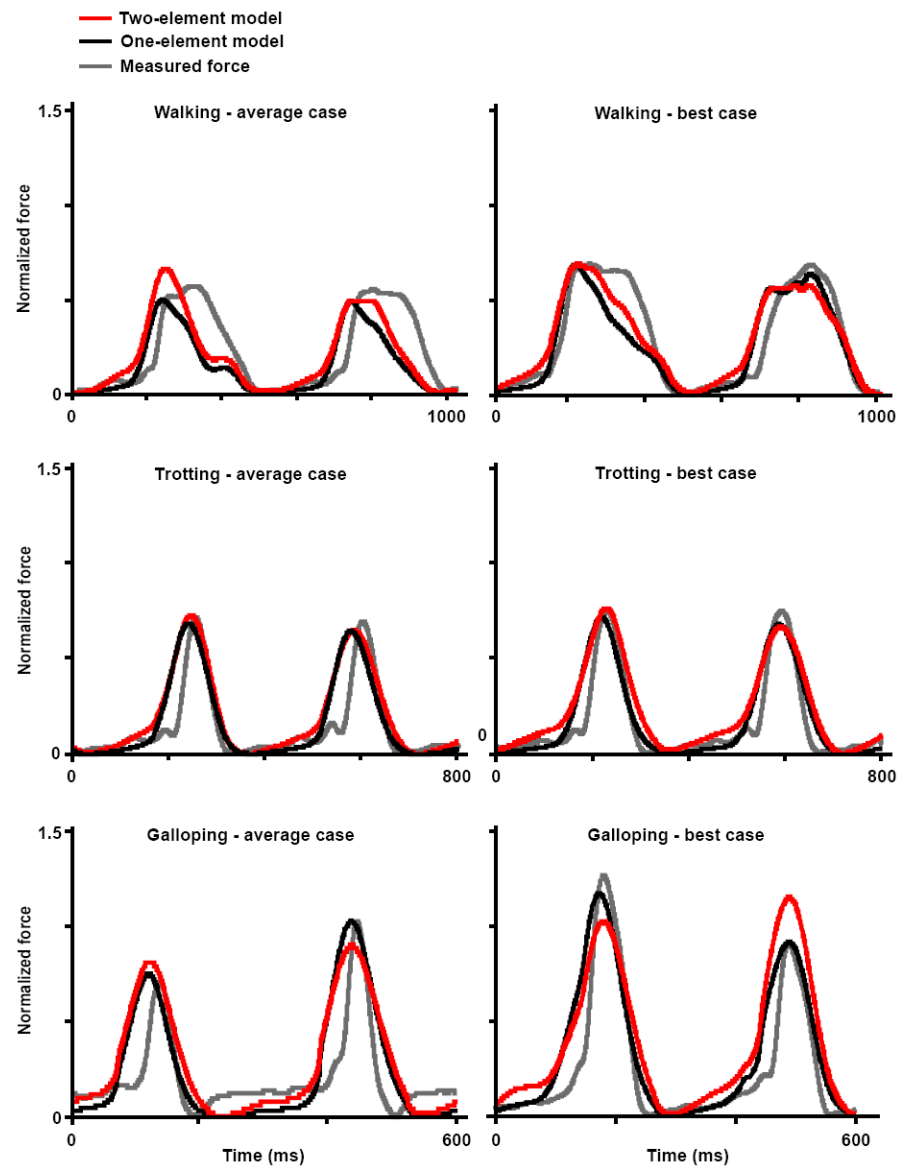
Figure 1.
Schematic representations of the one-element and two-element Hill-type models. Parameters outlined in dotted grey were taken from the literature; all other parameters were based on measured data. Contractile elements in the two-element model are formulated like the contractile element in the one-element model except that the activation and key parameters are specific to either slow or fast fibers. The active forces generated by the slow and fast elements are then summed to estimate the total active force. Refer to Table 3 for definitions of all symbols.
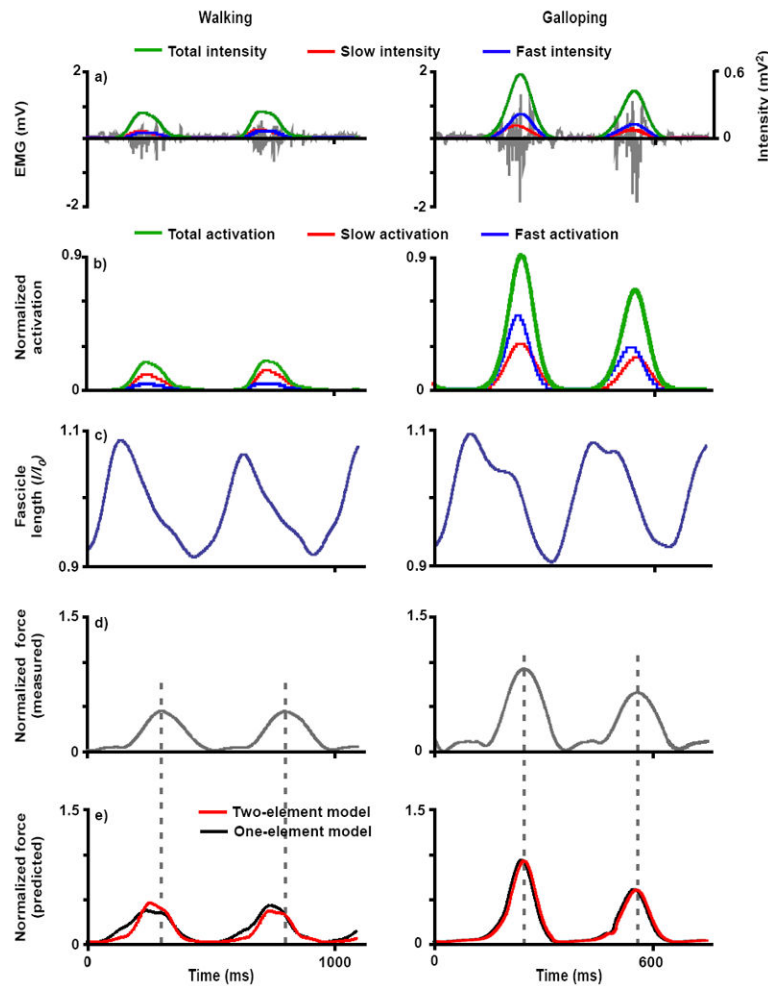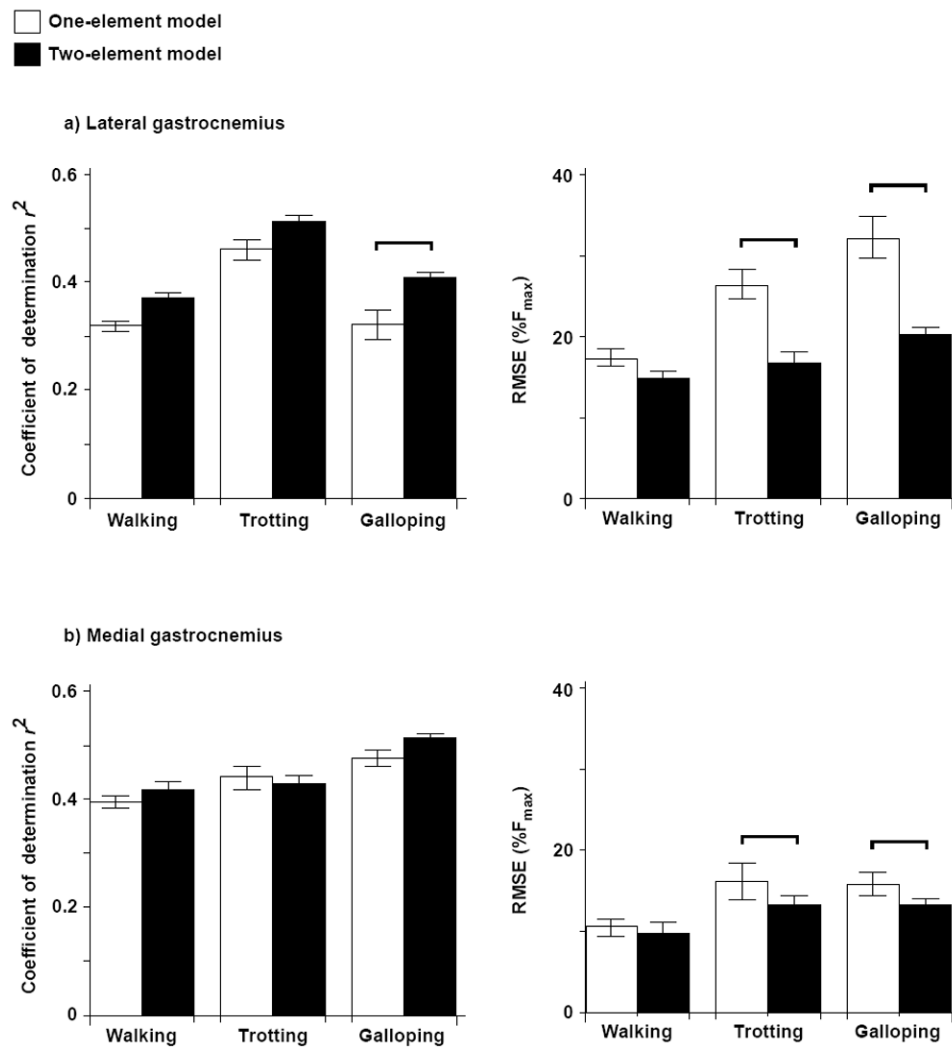
Figure 2.
Representative inputs and outputs of the one-element and two-element models for the goat LG muscle during walking and galloping: a) EMG (grey) and total (green), slow (red), and fast (blue) EMG intensity, b) total (green), slow (red), and fast (blue) activation normalized to maximum *in vivo* activation, c) fascicle length normalized to optimal resting length, d) measured tendon force normalized to maximum *in vivo* force, and e) muscle forces normalized to maximum *in vivo* force as predicted by the one-element model (black) and two-element model (red). These are representative trials from one goat. The dotted grey line indicates when the peak force occurs for each step.
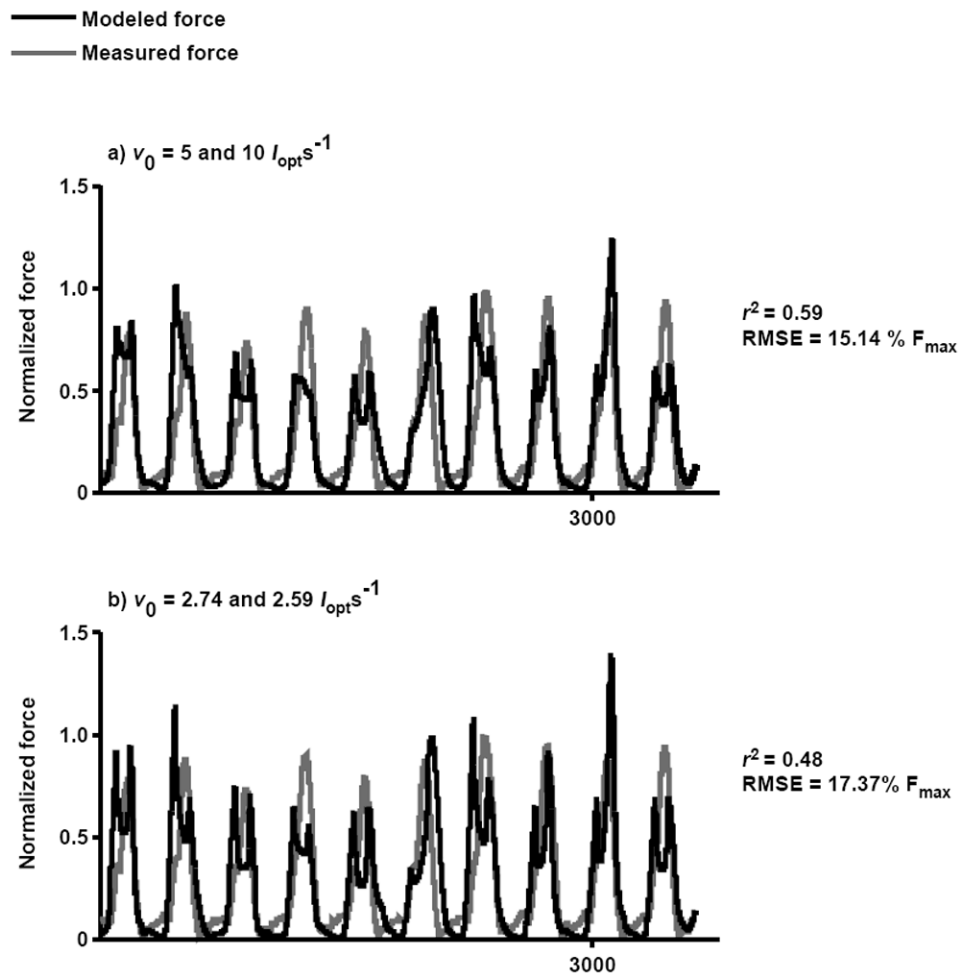
Figure 3.
Force profiles of the LG muscle during walking, trotting, and galloping. Measured forces (grey) and predicted forces from the one-element model (black) and two-element model (red) are shown for an average case (i.e., average r^2 and RMSE values) and for a "best" case. Models were assigned v_o values of 5 and 10 $l_{opt}s^{-1}$ for the slow and fast fibers, respectively, with a fiber-type proportion of 75% fast fibers. These are representative trials.

Figure 4.
Comparison of r^2 and RSME values for the one- and two-element models as determined for the different gait conditions and for the a) LG and b) MG muscles. Bars show the mean ± SEM pooled from all the goats. The two-element model was assigned v_o values of 5 and 10 $l_{opt}s^{-1}$ for the slow and fast fibers, respectively, with a fiber-type proportion of 75% fast fibers. *Post hoc* Tukey tests were conducted to identify significant differences between the models for each gait, and these differences are denoted by the horizontal bars.

Figure 5.
Sensitivity of predicted forces to maximum shortening velocity. The measured force is compared to the LG force predicted using the differential model assuming maximum shortening velocities of the slow and fast fibers to be: a) 5 and 10 $l_{opt}s^{-1}$ based on values from the literature and b) 2.74 and 3.59 $l_{opt}s^{-1}$ based on *in situ* measurements. The model was assigned a fiber-type proportion of 75% fast fibers. This is a representative trial with average r^2 and RMSE values from one goat during trotting.

Table 1

Constants for the transfer functions used to determine active state from EMG intensity (Eq. 1; see also Lee et al. 2011).

Constants	Total Intensity	Slow Motor Unit	Fast Motor Unit
τ_1	6.37	34.06	18.14
β_1	0.59	0.73	0.90
τ_2	38.05	36.27	20.91
β_2	0.76	0.74	0.99
τ_3	15.89	37.82	20.75
β_3	0.71	0.92	0.98
t_{off}	2.0	6.5	1.5

Table 2

Mean and standard deviation of muscle architectural parameters

Muscle	Resting fascicle length (mm)	Optimal fascicle length (mm)	Resting pennation angle (degree)
Lateral gastrocnemius	12.6 (1.5)	15.9 (4.2)	21.1 (4.5)
Medial gastrocnemius	13.4 (1.9)	17.0 (3.4)	24.3 (2.2)

Table 3

Parameters used in the muscle models.

Parameter	Definition	Source
$\hat{a}(t)$	Normalized, activation state of fibers	Derived from measured EMG
c	Scalar to calculate actual from normalized force	Measured
F_m	Muscle force	Calculated
F_{max}	Maximum *in vivo* force during incline trotting	Measured
$\bar{F}_p(l)$	Normalized, passive force-length relation	Measured (see Eq. 5)
$\bar{F}_a(l)$	Normalized, active force-length relation	Measured (see Eq. 4)
$\bar{F}_v(v)$	Normalized, force-velocity relation	Literature (see Eq. 6 and 7)
k	Curvature of force-velocity relation	Literature (0.29 and 0.18 for fast and slow fibers; Wakeling et al., 2012)
l	Fascicle length	Measured
v	Fascicle velocity	Derived from l
v_0	Maximum shortening velocity	Estimated (2.74 and 3.59 $l_{opt}s^{-1}$)
		Literature (5 and 10 $l_{opt}s^{-1}$)
θ	Pennation angle	Measured
p	Fractional area of the fast fibers	Literature (0.5 and 0.75)

Table 4

Force-velocity properties and activation state for the one- and two-element models.

Model	Force-velocity curvature, k	Maximum unloaded shortening velocity, v_0	Activation state
One-element	$k_{slow} + (k_{fast} - k_{slow})p$	$v_{o,slow} + (v_{o,fast} - v_{o,slow})\,\hat{a}(t)$	$\hat{a}(t)$
Two-element	k_{slow}	$v_{o,slow}$	$\hat{a}_{slow}(t)$
	k_{fast}	$v_{o,fast}$	$\hat{a}_{fast}(t)$